

## Supporting Information:

### Extensive H-atom abstraction from benzoate by OH-radicals at the air-water interface

Shinichi Enami<sup>a\*</sup>, Michael R. Hoffmann<sup>b</sup> and Agustín J. Colussi<sup>b\*</sup>

<sup>a</sup>*National Institute for Environmental Studies, Onogawa, Tsukuba, Ibaraki 305-8506, Japan*

<sup>b</sup>*Linde Center for Global Environmental Science, California Institute of Technology, California 91125,  
U.S.A*

---

\*Author to whom correspondence should be addressed: [enami.shinichi@nies.go.jp](mailto:enami.shinichi@nies.go.jp), phone: +81-29-850-2770 (S.E.) or [ajcoluss@caltech.edu](mailto:ajcoluss@caltech.edu) (A.J.C)

## SI Appendix

### SI Methods

Ozone is produced from ultrapure  $O_2(g)$  (purity > 99.995 %, Kyoto Teisan) flowing at 1.0 standard liters per minute through a high-pressure discharge ozonizer (KSQ-050, Kotohira).  $O_3(g)$  concentration is directly quantified online by a UV-Vis absorption spectrophotometry (Agilent 8453) at 250 nm and 300 nm, (absorption cross sections  $\sigma = 1.1 \times 10^{-17}$  and  $3.9 \times 10^{-19} \text{ cm}^2 \text{ molecule}^{-1}$ , respectively)<sup>1</sup> prior to entering the reaction chamber (Fig. S1). Throughout the text, the  $[O_3(g)]$  values correspond to the concentrations actually sensed by the microjets in the reaction chamber, which are  $\sim 10$  times smaller than those determined upstream UV absorbances due to dilution by the drying  $N_2$  gas.  $H_2O(g)$  is carried into the chamber via a known flow of  $N_2(g)$  saturated by sparging milli-Q water (Fig. S1). We assume that the chamber is saturated with  $H_2O(g)$  at 298 K throughout.

The 266 nm beam emitted by our  $Nd^{3+}$ :YAG laser setup (LOTIS TII, LS-2131M-10 with a harmonic generator assembly HG-TF, pulse duration  $8 \pm 1$  ns, 266 nm beam diameter  $10.0 \pm 1.0$  mm, beam divergence  $\leq 1.5$  mrad, 10 Hz) is used to generate  $\cdot OH(g)$  at or near the gas-liquid interface (Fig. S1). The 266 nm laser beam energies are measured with a power meter (OPHIR, NOVA II, sensor:3A-P-V1-ROHS). The 266 nm beam energy is controllable up to  $40 \text{ mJ pulse}^{-1}$ . The fate of  $O(^3P)$  is to react with  $O_2(g)$  to regenerate  $O_3$  within  $50 \mu\text{s}$  under present conditions. We previously demonstrated that the reaction of  $O(^1D)(g)$  with reactant(aq) is negligible.<sup>2, 3</sup> The laser beam is introduced into the spraying chamber via quartz prisms (synthetic fused silica, refractive index  $n_d = 1.458$ ) on kinematic prism holders (SIGMAKOKI Co., LTD., Japan)

and aligned with a He-Ne laser (Melles Griot, 05-LHP-111, 632.8 nm CW) beam, which becomes visual as it is scattered upon hitting the liquid jet.

Experimental conditions were as follows: drying gas flow rate: 12 L min<sup>-1</sup>; drying gas temperature: 340 °C; inlet voltage: + 3.5 kV relative to ground; fragmentor voltage value: 80 V. Benzoic acid (chemical purity >99.5 %) was purchased from Nacalai Tesque. D<sub>2</sub>O (isotopic purity >99.9 %) were purchased from Sigma-Aldrich. Benzoic acid-2,3,4,5,6-d<sub>5</sub> (chemical purity 98 %, isotopic purity 99.0 %) was purchased from Toronto Research Chemicals. All solutions were prepared in purified water (Resistivity ≥ 18.2 MΩ cm at 298 K) from a Millipore Milli-Q water purification system. The pH of the solutions were measured by a calibrated pH meter, Horiba LAQUA F-74, before each experiment.

### **Kinetic model calculations**

We performed numerical calculations on the model mechanism shown in Scheme 1 of the main text using *Mathematica* 10 software. Our calculations do not attempt to simulate experimental data, but to account in a semi-quantitative way the intriguing dependences of product yields on ·OH dose and benzoate concentrations on the basis of plausible kinetic parameters. Assumed rate constants used for numerical calculations are shown in Table S1.

**Table S1** Rate constants used for numerical calculations.

Rate constants
$k_{1AD} = 5 \times 10^{-12} \text{ cm}^{-3} (\text{molecule s})^{-1}$
$k_{1AB} = 7.5 \times 10^{-13} \text{ cm}^{-3} (\text{molecule s})^{-1}$
$k_{2A} = 1.7 \times 10^{-11} \text{ cm}^{-3} (\text{molecule s})^{-1}$
$k_{-2A} = 200 \text{ s}^{-1}$
$k_{2B} = 1.5 \times 10^{-12} \text{ cm}^{-3} (\text{molecule s})^{-1}$
$k_3 = 1.7 \times 10^{-11} \text{ cm}^{-3} (\text{molecule s})^{-1}$
$k_4 = 5 \times 10^{-12} \text{ cm}^{-3} (\text{molecule s})^{-1}$
$k_5 = 1.7 \times 10^{-11} \text{ cm}^{-3} (\text{molecule s})^{-1}$
$k_{-5} = 200 \text{ s}^{-1}$
$k_6 = 5 \times 10^{-12} \text{ cm}^{-3} (\text{molecule s})^{-1}$
$k_7 = 1.7 \times 10^{-11} \text{ cm}^{-3} (\text{molecule s})^{-1}$

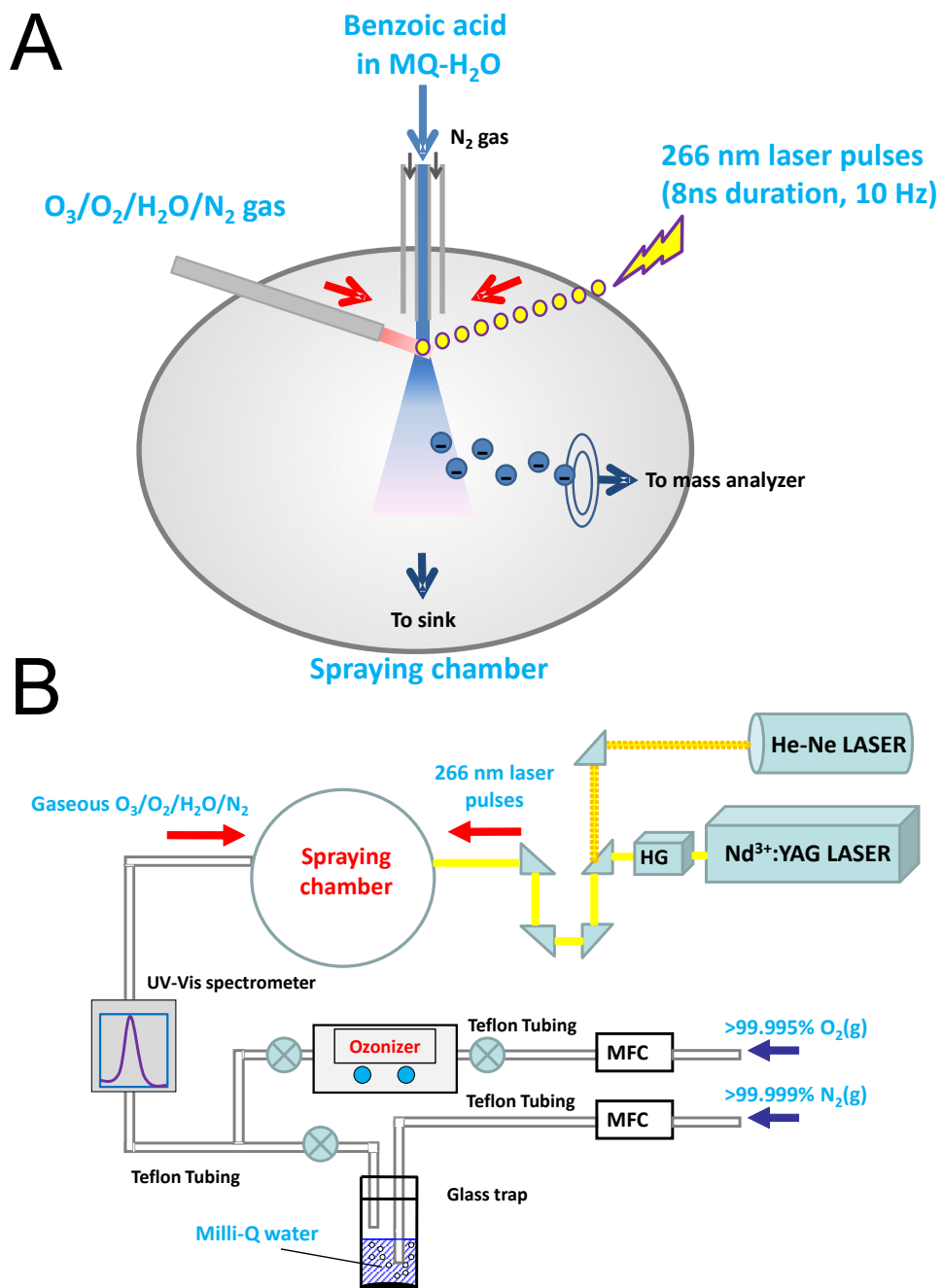


**Figure S1** – Schematic diagram of an in-situ measurement of  $\cdot\text{OH}$ -radical reaction with benzoate at the air-water interface. HG stands for harmonic generator. MFC stands for mass flow controller.

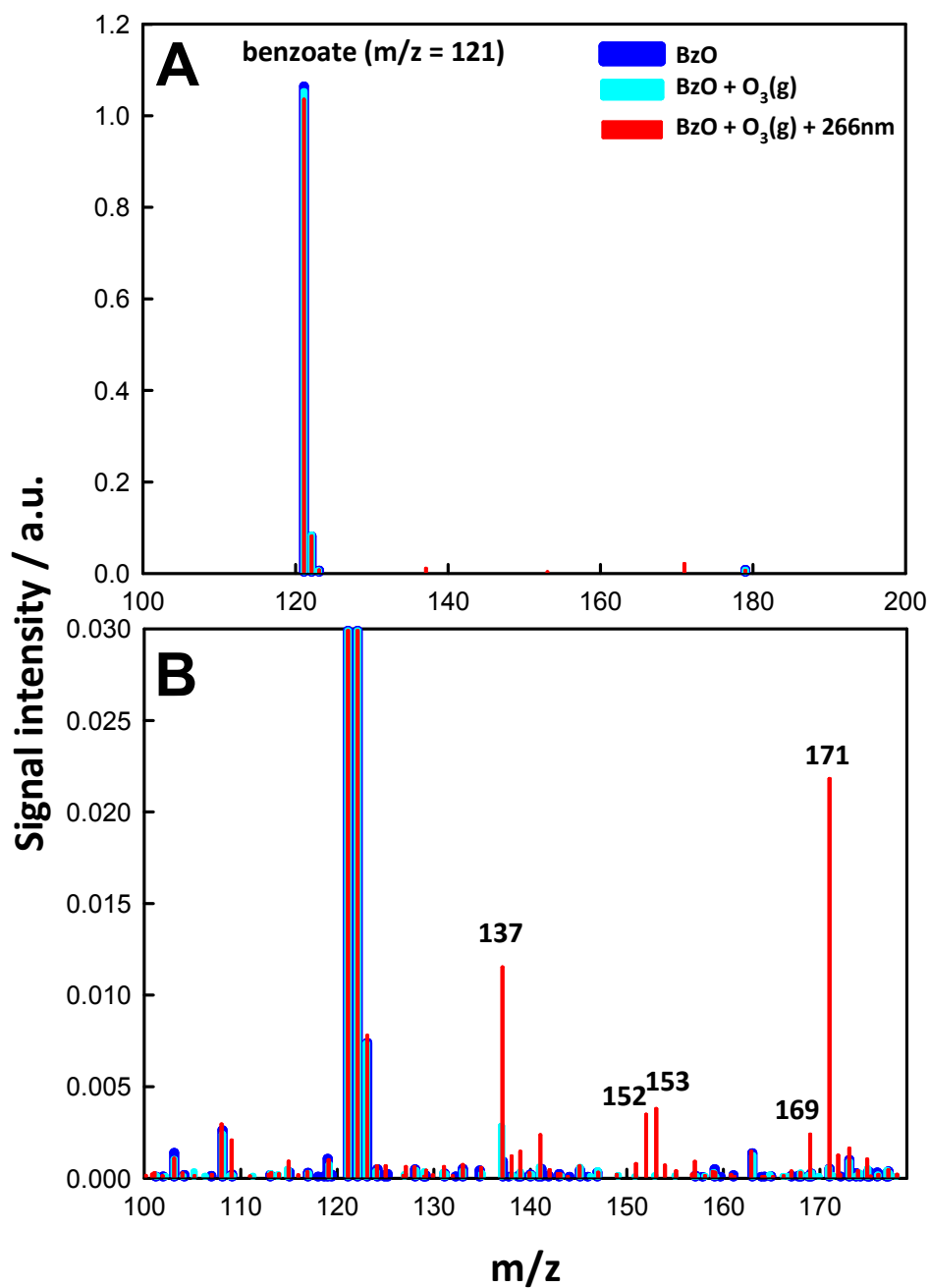


**Figure S2** – A) Negative ion electrospray mass spectra of 1.0 mM (pH 4.0) benzoic acid microjets in the absence (blue) or presence of  $2.4 \times 10^{15}$  molecules  $cm^{-3}$   $O_3(g)$  with the 266 nm laser pulses (40 mJ,  $\sim 8$  ns nm, 10 Hz) off (cyan) or on (red). B) Zooming in spectra. Note that the presence of  $O_3(g)$  without light (cyan) does not generate new product signals.

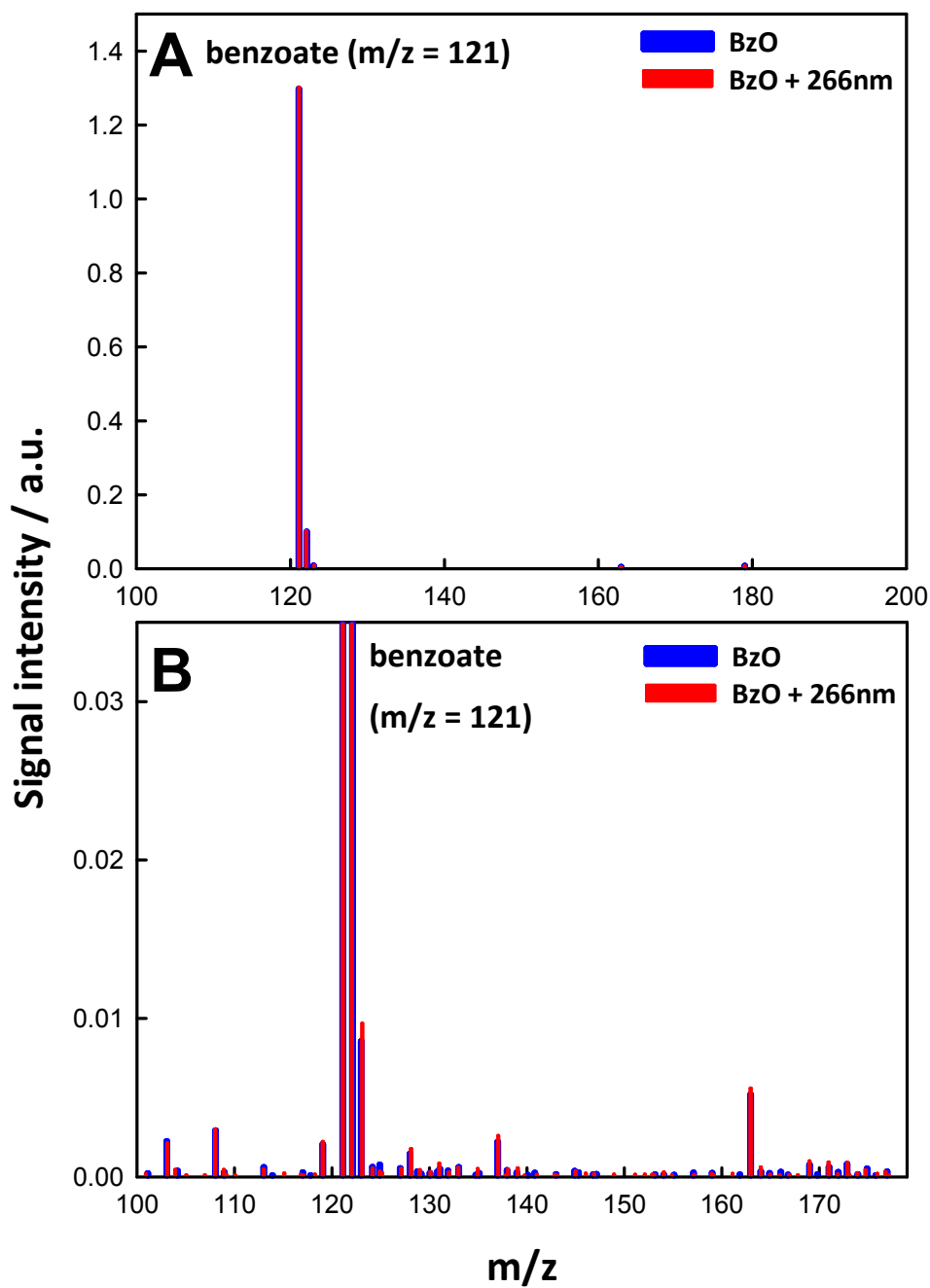


**Figure S3** – A) Negative ion electrospray mass spectra of 1.0 mM (pH 4.0) benzoic acid microjets in the absence (blue) or presence (red) of 266 nm laser irradiation ( $40 \text{ mJ pulse}^{-1}$ ) at 1 atm and 298 K under no  $\text{O}_3(\text{g})$  conditions. B) Zooming in spectra

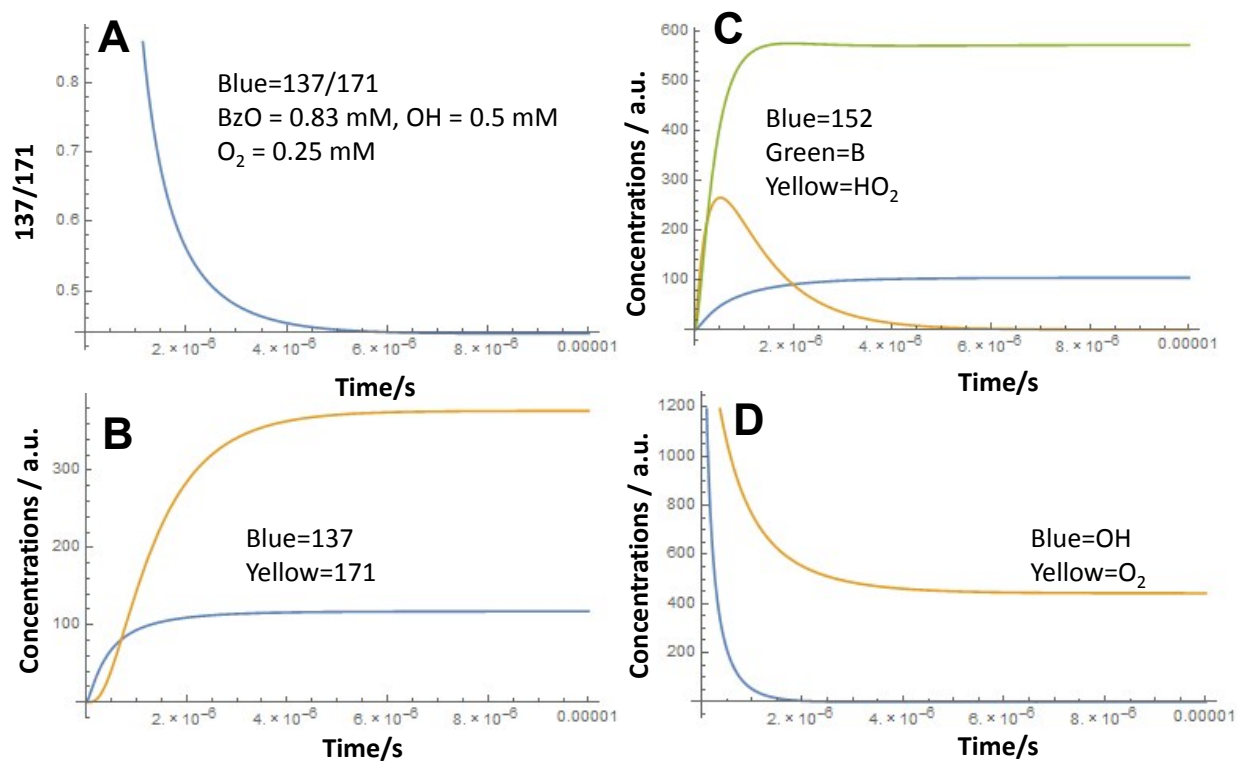


**Figure S4** – Results of numerical calculations on the model mechanism. A) The 137/171 ratio of signal intensities, B) concentration profiles of the products at  $m/z = 137$  and  $171$ , C) concentration profiles of HO<sub>2</sub> and the  $m/z = 152$  and B products (see main text), D) concentration profiles of OH-radical and O<sub>2</sub>, as functions of time.



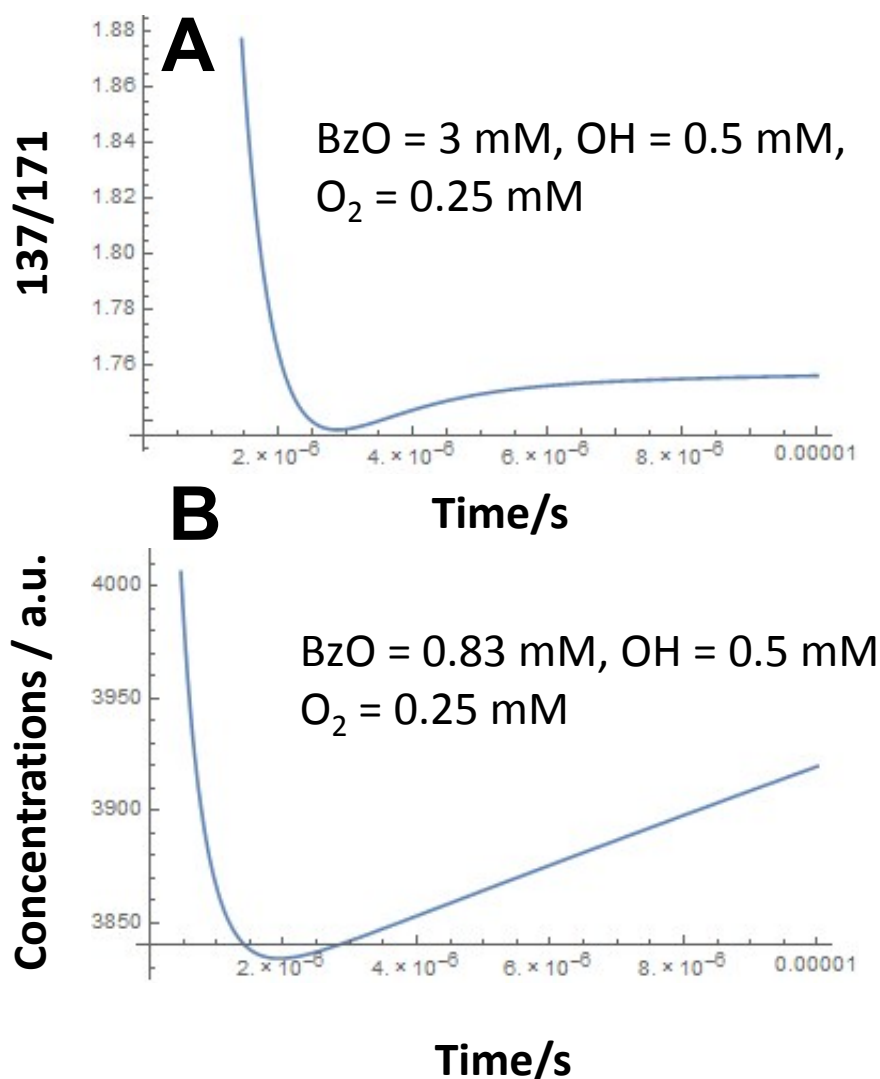


**Figure S5** – Results of numerical calculations on the model mechanism. A) The 137/171 ratio of signal intensities, B) concentration profiles of benzoate as functions of time per second. Benzoate concentration rebounds via diffusion from the bulk into the monitored interfacial layers after the chemical processing is over, a phenomenon that accounts for the observed non-exponential [BzO] decay profiles as function of pulse energy (see main text).

## SI REFERENCES

1. S. P. Sander, R. R. Friedl, W. B. DeMore, A. R. Ravishankara, D. M. Golden, C. E. Kolb, M. J. Kurylo, R. F. Hampson, R. E. Huie, M. J. Molina and G. K. Moortgat, *Chemical Kinetics and Photochemical Data for Use in Stratospheric Modeling Supplement to Evaluation 12: Update of Key Reactions Evaluation Number 13*, 2000.
2. S. Enami, M. R. Hoffmann and A. J. Colussi, *J. Phys. Chem. Lett.*, 2015, **6**, 527-534.
3. S. Enami, M. R. Hoffmann and A. J. Colussi, *J. Phys. Chem. A*, 2014, **118**, 4130-4137.